J Mater Sci (2023) 58:983–995

Polymers & biopolymers

The holographic properties of photopolymers on the base of oxygen- and sulfur-containing spirocyclic monomers

Vladimir Shelkovnikov[1], Evgenii Vasiliev[1,*], Dmitry Derevyanko[1], Alexandra Bukhtoyarova[1], Viktoria Berezhnaya[1], and Inna Shundrina[1]

[1] *Novosibirsk Institute of Organic Chemistry, Siberian Branch of the Russian Academy of Science, 9, Academician Lavrentjev Ave, Novosibirsk 630090, Russia*

Received: 2 September 2022
Accepted: 17 December 2022
Published online: 2 January 2023

ABSTRACT

The influence of the oxygen and sulfur atoms in the spirocycles (–O–CH_2–CH_2–O–, –O–CH_2–CH_2–S–, –S–CH_2–CH_2–S–) of the spirocyclic acryloylpiperidonyl monomers on the thermomechanical and holographic properties of the photopolymer material was studied. The conversion of double bonds of monomers during UV polymerization was determined by IR spectroscopy method. The refractive indices of spirocyclic monomers and photopolymers were measured. The phase transmission diffraction gratings were recorded in photopolymer materials containing the spirocyclic monomers. The highest modulation of the refractive index was observed in the photopolymer based on the acryloylpiperidonyl dithiaazaspiroheterocyclic (–S–CH_2–CH_2–S–) monomer. It was shown that light scattering in the photopolymer at hologram recording has noticeable negative contribution and for the decrease in the diffraction efficiency of holograms. The phase incompatibility of the polymer matrix and formed photopolymer is considered as the reason of the light-scattering growth.

Handling Editor: Maude Jimenez.

Address correspondence to E-mail: vev@nioch.nsc.ru

https://doi.org/10.1007/s10853-022-08105-8

GRAPHICAL ABSTRACT

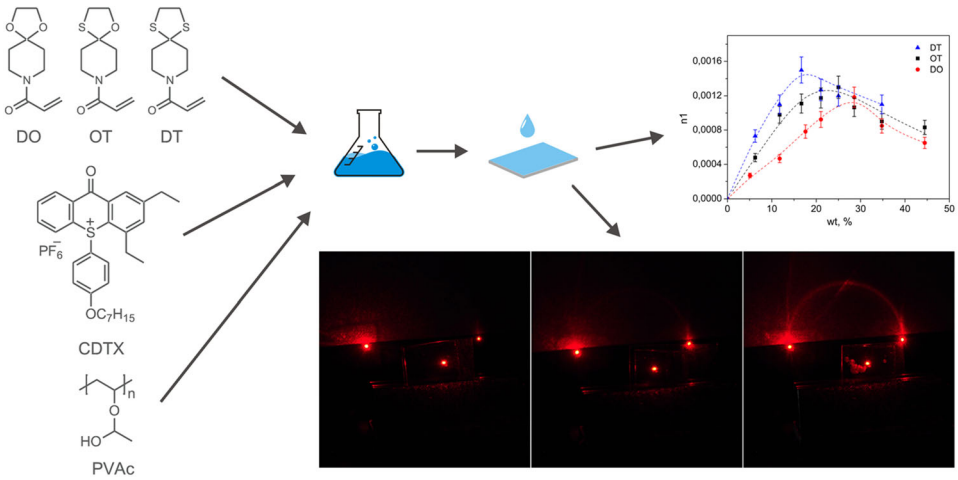

Introduction

Holographic photopolymer materials (HPMs) are required in many optical applications: holographic image recording [1], security and anti-counterfeit signs [2], holographic data storage systems [3], optical elements, interferometry [4, 5]. Among the many well-known holographic materials, HPM has a number of advantages: low cost, optical transparency, and simple post-processing [6].

Usually, HPM film consists of a polymer binder, monomers, and a photoinitiation system [7]. The photoinitiating system used is the cationic derivative of thioxanthenone, which effectively initiates the polymerization of acrylates [8] when exposure by radiation with a wavelength of 375 nm. According to the mechanism of photodecomposition of sulfonium salts [9, 10], the intermediates of both the radical and the cationic type form as the reaction products during photolysis of the cationic derivative of thioxanthenone. These radicals initiate polymerization of the acrylate monomers according to free radical polymerization (FRP) mechanism [11–13]. Further, photoinitiated polymerization occurs according to the classical scheme with the stages of propagation and termination of polymerization [14, 15].

Exposure of the HPM in accordance with the harmonic interference pattern formed by coherent laser beams occurs when an elementary hologram (a phase transmittance diffraction grating) is recorded into the photopolymer. The process of the monomer polymerization is initiated in the exposed fingers, while this does not occur in the dark fingers. The refractive index (RI) modulation between the polymerized and unpolymerized fingers is a basis for the hologram formation. The difference in refractive indices between the polymer binder and the polymer formed from the monomer as result of photopolymerization defines the diffraction efficiency (DE) of holograms according the Kogelnik equation for the case of a phase diffraction grating, under the Bragg conditions [16]:

$$\mathrm{DE} = \sin^2\left[\frac{\pi n_1 d}{\lambda \cos\theta}\right] \quad (1)$$

where n_1 is RI modulation (half of difference in refractive indices), d is the thickness of the grating; λ is the beam wavelength; θ is the angle between the wave vector of the beam and the normal to the grating surface.

One of the ways to improve HPM is the synthesis of monomers with a high refractive index [17, 18], which should lead to an increase in the refractive index modulation between the polymer binder and the new polymer. Similar monomers are obtained by introducing atoms with increased molar refraction

into their structure, for example, these are sulfur atoms [19]. During photopolymerization, nanoscale structures of the new polymer are formed in the binder, as a rule, in the form of scatter centers. The size and refractive index of the polymer scatter centers affect the light scattering of the hologram. An increase in light scattering in HPM should be expected based on the fluctuation nature of Rayleigh scattering of linearly polarized light on inhomogeneous polymer structures. This is due to the increase the RI of the new polymer and an increase in the size of the formed structures, in addition to an increase of the diffraction efficiency. The decrease in the thermodynamic compatibility of the binder polymer and the new polymer and, as result, their phase separation will also lead to an increase in light scattering in the HPM [20]. In this regard, the use of monomers containing highly refractive heteroatoms other than binder atoms can raise the requirements for the compatibility of a new polymer with a polymer binder. As a rule, when developing methods for improving a photopolymer by introducing highly refractive atoms into the monomer structure, the change in light scattering or the compatibility of two interpenetrating polymer nets is not taken into account.

The concept of the development of holographic photopolymer materials implies a comprehensive study of the influence of the HPM components on the properties of the recording medium. Three monomers—acryloyl derivatives of 4-piperidone with different numbers of sulfur and oxygen atoms in spirocycles with the same acrylamide part: DO, OT, and DT—were synthesized (Fig. 1). These monomers contained atoms with different polarizabilities and, accordingly, with different molar refractions, and were used to estimation the influence of the structure of monomers on the relative light scattering in the HPM.

The goal of this research is to determine the effect of oxygen and sulfur atoms in the spirocyclic monomers on the refractive, thermal, holographic, and light-scattering properties in HPM.

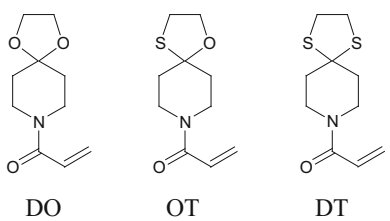

Figure 1 Structures of monomers.

Experimental

Materials

Poly (vinyl acetate) (Mw ~ 500,000 by GPC, CAS: 9003-20-7, Sigma-Aldrich) was used as polymer binder without purification. The monomers (Fig. 1) were acryloyl azaspiroheterocyclic derivatives of 4-piperidone (DO, OT, and DT). The synthesis of the DT monomer is published in [21], DO in [22]. OT was obtained by analogy with DT [21].

2,4-Diethyl-9-oxo-10-(4-heptyloxyphenyl)-9H-thioxanthenium hexafluorophosphate (CDTX) (Fig. 2) was used as the photoinitiator for holographic recording [23].

Preparation of the HPM

On the basis of the synthesized monomers, photopolymer compositions were obtained. The composition is a solution of a photoinitiator, a monomer, and a polymer binder in chloroform, at various molar ratios of reagents. For each experiment, the specific ratios of reagents are indicated below.

Polyvinyl acetate was chosen as a matrix in which the initial monomers are well dissolved during the preparation of HPM. No plasticizers were used in HPM to minimize the contribution of monomer diffusion to the diffraction efficiency of the holograms. As a photoinitiator, we used a cationic derivative of thioxanthenone, which has weak absorption at the recording wavelength in the UV region of the

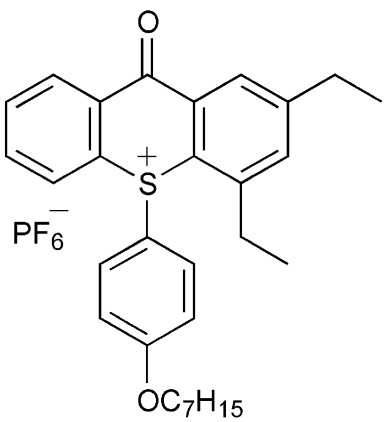

Figure 2 Structure of CDTX.

spectrum. This approach made it possible to form holograms with minimal distortion caused by the absorption of the medium. The holograms were recorded using UV radiation from a DPSS laser with a wavelength of 375 nm, which allowed the maximum manifestation of the features of Rayleigh scattering in HPM.

Photopolymer compositions were coated to the glass substrates arranged horizontally by slot-die coating method. Glass plates with photopolymer were dried at room conditions (25 °C, humidity 45%) for 15–18 h. As a result, the experimental samples with HPM layers of various thicknesses were obtained. Photopolymer films were covered with PET film to exclude oxygen inhibition of radical polymerization.

Obtained HPM makes it possible to exclude diffusion due to intentional absent of any plasticizer and absorption effects. HPM was prepared as the model samples which allow focusing on the influence of the difference in the refractive indices of new polymers and binder.

Preparation of the polymer films

UV-cured polymer films with a thickness of 300–400 μm were prepared from synthesized monomers to measure the RI of polymers and for TGA and DSC experiments. UV curing of the samples was carried out by ELC-410 UV Spot Cure System (Electro-Light Corporation) for 30 min at distance of 10 mm. Then the samples were kept in a vacuum (0.1 atm.) at a temperature of 70 °C for a day to increase the monomer conversion.

Polymer films for DMA analysis were used too. In this case, polymer films (PVAc binder: monomer about 1:1) were UV-cured whole and kept in vacuum the same way.

Polymer films with a thickness of 10 μm on a KBr substrate were prepared in a similar way to measure the degree of the monomer conversion by IR spectroscopy.

Analytical instruments

Fourier transform-infrared (FT-IR) spectra were obtained using KBr disk on a 640-IR, Varian, USA (resolution of 0.25 cm^{-1}, 400–7000 cm^{-1}) at room temperature.

Abbe refractometer DR-M4 (Atago) was used to measure RIs. The RIs of viscous monomers (DO and OT) were measured directly according to a standard measurement procedure. The RIs of powder monomer (DT) were measured in a DMSO solution according to the procedure described in [24]. The RIs of polymer films were measured using an immersion liquid α-bromonaphthalene (CAS: 90-11-9, n = 1.659).

Interferometer MII-4 (Lomo) was used to measure film thicknesses less than 10 microns by the interferometric method.

Thermogravimetric analysis (TGA) and differential scanning calorimetry (DSC) measurements were performed using a NETZSCH STA 409 instrument at a heating rate of 10 °C/min under He flow. T_g was determined in the DSC curves as the center of the step transition in the second heating run. The short-term thermal stability of copolymers was estimated from the 3% weight loss temperatures ($T_{3\%}$) using TGA. Dynamic mechanical analysis (DMA) measurements were performed on a DMA 242 C NETZSCH instrument. The experiments were carried out using the tension mode of the DMA instrument over the temperature range from − 50 to 150 °C with 3 °C/min heating rate under He flow. The 10-mm strips of films were scanned at a frequency of 1 Hz and 10 μ peak-to-peak oscillation amplitude that was well within the linear viscoelastic region.

Holographic experimental setup

The two-beam interference experimental setup (Fig. 3) described in detail in [25] was used for CW recording of holographic gratings. The phase

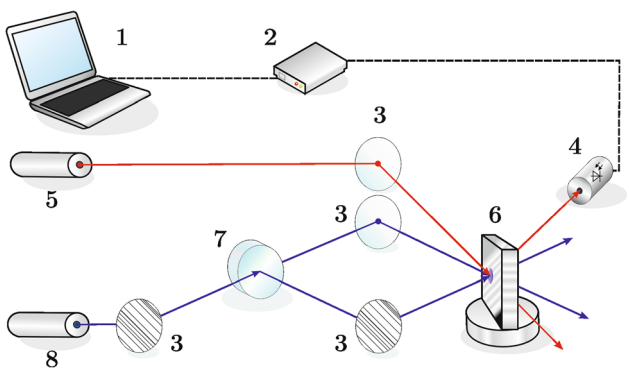

Figure 3 Holographic experimental setup. 1—computer; 2—power meter Thorlabs PM100USB; 3—mirrors; 4—sensor Thorlabs S121C; 5—CW He–Ne laser (633 nm); 6—sample; 7—beam splitter; 8—CW DPSS laser (375 nm).

transmission holograms were recorded by a CW DPSS laser (8) (λ = 375 nm) with an intensity of 140 mW/cm^2. The laser beam was divided into two beams of equal intensity using a dichroic mirror (7), and then these beams were directed by mirrors (3) to the experimental sample (6) at the recording point of the hologram. Two laser beams formed sinusoidal holographic grating (square 1 mm^2) with the spatial frequency of 1250 lines/mm. The laser beam from a testing CW He–Ne laser (5) (λ = 633 nm, 0.5 mW) was directed to the same recording point. The DE kinetic dependences of the holograms were monitored by measuring the intensity of the diffracted beam of the He–Ne laser using a power meter (4). Measurement results were collected on a computer (1). The DE of each recorded hologram was calculated as the ratio of the diffracted beam power (P_d) to the sum of the powers of the diffracted and transmitted beams (P_t).

Results and discussion

Estimation of the conversion degree of the acrylate groups by FT-IR spectroscopy

FT-IR spectroscopy methods were applied to estimation of the conversion degree of double bonds of monomers as a result of exposure to UV radiation [26, 27]. Figure 4 shows the IR spectrum of a polymer film obtained from DO monomer before and after curing.

The IR spectrum of a non-cyclic analogue of the studied monomers, acrylamide, was considered in [28]. The peaks corresponding to out-of-plane deformation (torsion) vibrations of C–H bonds in the vinyl group of the molecule at 810 cm^{-1} [29], and stretching vibrations of the double bond C = C at 1612 cm^{-1} [29, 30] decrease during polymerization. Figure 4 shows similar peaks for the studied monomers: 794 and 1612 cm^{-1}, respectively.

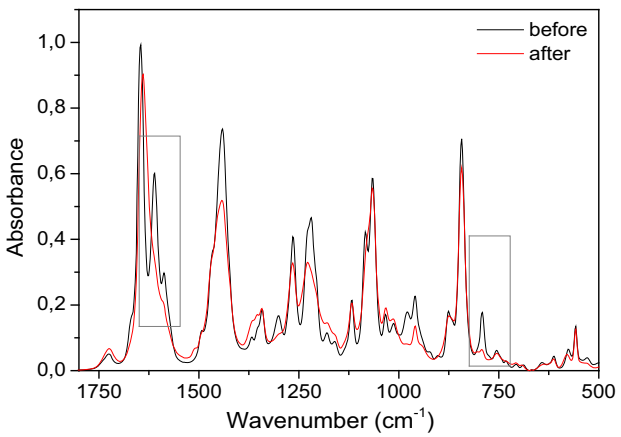

Figure 4 IR absorption spectra for the DO monomer before and after curing.

The absorption band at 1612 cm^{-1} was excluded from consideration because of the significant overlap with other vibration bands. The absorption band at 794 cm^{-1} was chosen to calculate the conversion degree of monomers (C, %) [26]:

$$C(\%) = \left(1 - \frac{(A_{C=C})_{afterexposure}}{(A_{C=C})_{beforeexposure}}\right)100\%, \quad (2)$$

where $(A_{C=C})_{before\ exposure}$ and $(A_{C=C})_{after\ exposure}$—integral vibrations at 794 cm^{-1} before and after UV curing, respectively.

The DO polymer film had a conversion degree of C = 77%, OT polymer film had C = 82%, and DT polymer film had C = 74%. The cured HPM films had a conversion degree of monomer in the PVAc binder about C_{DO} = 68%, C_{OT} = 72% and C_{DT} = 69%.

Thermal property of polymers

Thermal behavior of polymers was evaluated by TG and DSC. Polymers formed from DO, OT, and DT monomers have glass transition temperatures of 139, 130, and 155 °C, respectively. Since the cured polymers are practically insoluble in organic solvents, they were not purified from residual monomers. The polymer formed from the powder DT monomer has the highest glass transition temperature in spite of the lower conversion. It should be noted that the glass transition temperature of DO, OT, and DT polymers is significantly higher than the T_g of PVAc ($\sim$ 30 °C), which is used as the HPM binder. The polymers indicated good thermal stability. The 3% weight loss temperatures of these polymers were 224, 220, and 263 °C correspondently.

Spectra of monomers and polymers

The transparency of optical polymers is one of the key parameters that determine their practical applicability. Figure 5 shows the transmission spectrum of a 400 μm thickness polymer film formed from a DT monomer. The polymer has a high transparency in the range of 350–800 nm. Polymer films formed from

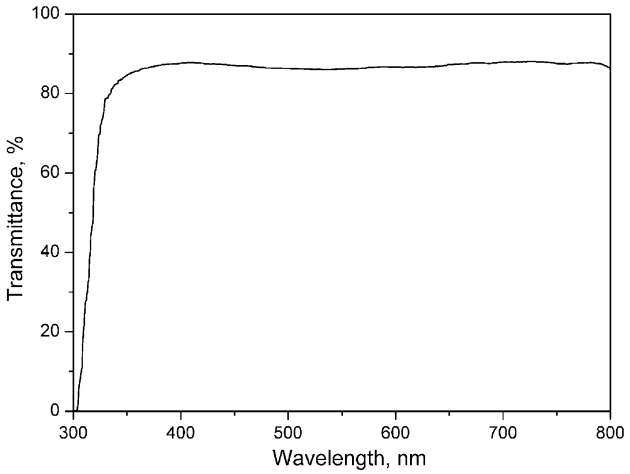

Figure 5 Transmission spectrum of a polymer film formed from DT monomer relative to air.

DO and OT monomers have practically the same transmission spectra. These polymers can be used to create components for diffractive, micro-optical, and integrated-optical elements which operate in the near UV and visible spectral regions.

The photoinitiator of the HPM has a weak absorption band in the region of 350–400 nm (Fig. 6). This weak absorption band can be clearly seen in the inset of Fig. 6 on a logarithmic scale. Photoinitiator CDTX initiates polymerization of acrylic monomers by a free radical mechanism [31]. The extinction coefficient of CDTX in this band is 300–600 M^{-1} cm^{-1}. Thus, industrial sources of UV radiation with wavelengths of 365 and 405 nm [32] can be used to cure the films. Figure 7 shows the absorption spectra of HPM films formed from DO, OT, and DT monomers and sensitized by CDTX. The thicknesses of HPM films are about 60–70 μm. Recording of holographic optical elements and holograms into these photopolymer films is possible by UV radiation.

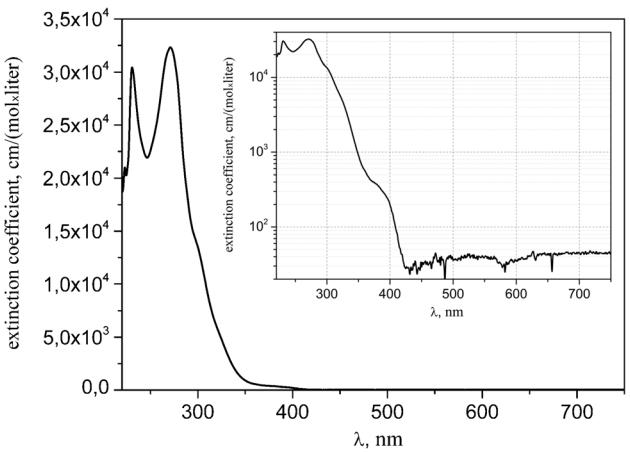

Figure 6 Absorption spectrum of CDTX in acetonitrile (the inset shows the absorption spectrum in logarithmic scale).

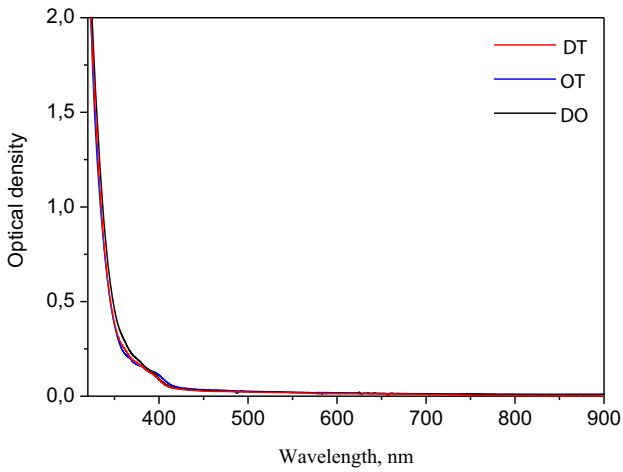

Figure 7 Absorption spectra of HPM films.

Refractive indices

Refractive index is an important parameter that determines the suitability of monomers and polymers for the development of the photonics optical elements. Table 1 shows the measured RIs of the DO, OT, and DT monomers.

It can be concluded that the replacement of one oxygen by sulfur in the structure of the synthesized monomer leads to an increase in the refractive index of the polymer by ~ 0.04.

A decrease in chromatic aberrations at the fabrication of optical elements based on the proposed polymers is important for practical applications in addition to the RI. Smaller chromatic aberrations are characterized by large values of the Abbe number, which is estimated from the refractive indices at wavelengths corresponding to the Fraunhofer lines C (656.3 nm), D (589.2 nm), and F (486.1 nm). For DT monomer and DT polymer, the RIs were measured at these wavelengths (Table 2). The Abbe number of the DT polymer was $V = 39$. In the Abbe diagram, the DT polymer falls into the area of Barium dense flints, which is preferable in the manufacture of polymer optics, waveguides, sealing compounds for LEDs and holographic optical elements in comparison with acrylic polymer or polycarbonate which are dense flints [33].

Table 1 RIs of the studied compounds

#	Name	$n^{25}{}_{D\ (monomer)}$	$n^{25}{}_{D\ (polymer)}$	Δn
DO	1-(1,4-Dioxa-8-azaspiro[4.5]decan-8-yl)prop-2-en-1-one	1.5125 ± 0.0009	1.5433 ± 0.0018	0.0308 ± 0.0027
OT	1-(1,4-Oxathia-8-azaspiro[4.5]decan-8-yl)prop-2-en-1-one	1.5538 ± 0.0006	1.5818 ± 0.0017	0.028 ± 0.0023
DT	1-(1,4-Dithia-8-azaspiro[4.5]decan-8-yl)prop-2-en-1-one	1.583 ± 0.003	1.630 ± 0.005	0.047 ± 0.005

Table 2 RIs of the DT monomer and DT polymer correspond to the Fraunhofer lines

Fraunhofer line	Wavelength (nm)	$n^{25}{}_{D\ (monomer)}$	$n^{25}{}_{D\ (polymer)}$
D	589	1.583 ± 0.003	1.630 ± 0.005
F	486	1.593 ± 0.003	1.642 ± 0.002
C	656	1.574 ± 0.005	1.626 ± 0.001

Holographic characterization study.

Transmittance phase gratings were recorded into a photopolymer with various monomers on an experimental UV recording setup [6]. The dynamics of grating formation was registered as the dependence of the DE on the exposure time. Figure 8 shows such a typical time dependence of the DE. The DE curve reaches a steady-state value during this time.

Modulations of the RI of phase diffraction gratings were calculated using the Kogelnik Eq. (1) from the recorded steady-state DEs. Modulation of the RI makes it possible to exclude different thicknesses of photopolymer layers and to estimate the efficiency of monomers polymerization under equal conditions. Figure 9 shows the RI modulation in the photopolymer layer depending on the mass fraction of monomers $C_{wt.\%} = m_{monomer}/(m_{monomer} + m_{PVA}) \times 100\%$).

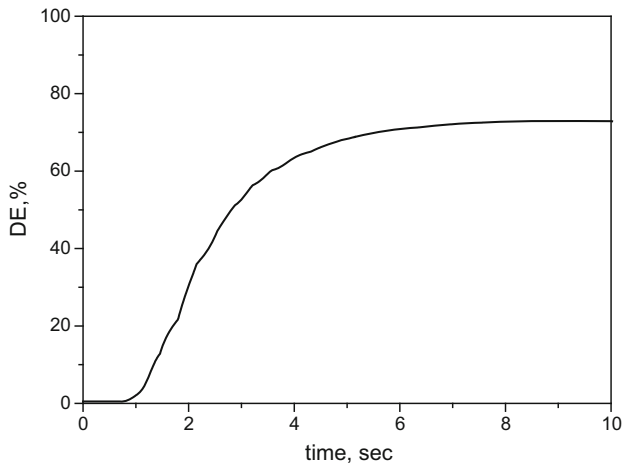

Figure 8 DE dependence of the hologram in a sample with 25 wt.% DT monomer (sample thickness 90 μm).

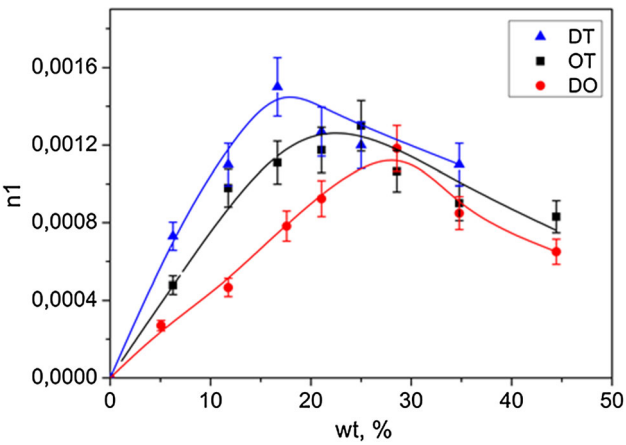

Figure 9 Modulation of RIs dependencies on the mass fraction of monomers in the layer.

It can be seen from the graph that the maximum n_1 was achieved when the photopolymer contained 20–30 wt.% monomer. Moreover, for the DT monomer, this fraction was 18 wt.%, OT—25 wt.%, and DO—30 wt.%. This difference is primarily caused by the different phase state of the monomers: DT monomer is a solid powder, while DO and OT monomers have an oily state at room conditions. Monomers have different RI, and their introduction into the photopolymer composition in fractions of 0–20 wt.% gives different efficiency. This is reflected in the different slopes of the curves in Fig. 9 in the range 0–20 wt.%. The maximum modulation of RI is achieved at the fraction of 20 wt.% DT monomer, and a further increase in the monomer concentration in the photopolymer only leads to a decrease in the

polymerization efficiency. Apparently, this is due to a significant decrease in the free volume of the interpenetrating polymer networks and, as a consequence, to a decrease in the rate of the polymerization reaction. When more than 35 wt.% monomer is added to the DT photopolymer, crystallization of the samples occurs. In the case of DO and OT monomers, the free volume limitations do not affect until 45 wt.% of monomer, because they have less diffusion limitations and provide the growth of n_1. However, the photopolymer layer becomes excessively plastic with a further increase in the monomer fraction. This leads to degradation of the diffraction grating and a decrease in the steady state n_1 at the fraction of more than 40 wt.% (Fig. 9).

Light scattering by the diffraction grating

Photopolymer with various monomers showed an increase in the light scattering of the material in the DO–OT–DT series in parallel with an increase in the modulation of the RI of the gratings. An increase in the light scattering of the photopolymer reduces the DE of the gratings and limits the resolution of the recording media. Light scattering leads to the appearance of the effect of non-local initiation of the photopolymerization process. "Noise holographic gratings" caused by the interference of scattered and incident light in this case are formed [34, 35]. These gratings are observed as a light circle between the transmitted and diffracted beams (Fig. 10).

Figure 10 A photo of the diffraction pattern of a hologram recorded in a photopolymer with a DT monomer.

Figure 11 shows photo of diffraction patterns from holograms recorded in photopolymer layers containing DO-, OT-, and DT monomers. Minimal light scattering is observed in the case of a photopolymer with DO monomer (Fig. 11a). The photopolymer with OT monomer showed an increase in light scattering and the appearance of weak circular scattering between zero and first diffraction orders (Fig. 11b). Photopolymer with DT monomer provides noticeable circular scattering between zero and first diffraction orders (Fig. 11c). Figure 12 shows the curves of the relative scattered light intensity in the region of the zero diffraction order. A significant change in the scattered light intensity in the series of monomers: DO–OT–DT is also observed. Greater light scattering leads to a more intense formation of noise holographic gratings, on which a part of the active components is consumed. The formation of noise gratings is a negative process that leads to a decrease of the first-order diffraction efficiency. A possible reason for this may be the incompatibility of the polymer binder and polymers formed from monomers. The films of cured monomers in a polyvinyl acetate binder (1:1 wt.%) were investigated by DMA methods. The storage modulus (E'), loss modulus (E''), and loss tangent ($tg\delta$) were recorded as functions of temperature (see Fig. 13). According to IR spectroscopy data, the conversion degree of the DO monomer in the PVAc film was 68%, the OT monomer in the PVAc film was 72%, and the DT monomer in the PVAc film was 69%.

The maxima on the plots of the loss modulus E'' and the tangent of the angle of mechanical losses $tg\delta$ are associated with glass transitions in the polymer material. The phase morphology of polymer materials based on polymer mixtures depends on their compatibility. For compatible polymers, a single glass transition temperature is observed, which is close to the additive values depending on the composition. Mixtures of two incompatible polymers have two glass transition temperatures, which do not change depending on the composition and correspond to homopolymers. Mixtures of two partially compatible polymers have two or three glass transition temperatures and can differ significantly from the glass transition temperatures of homopolymers. The third glass transition temperature is associated with the formation of a significant fraction of the interfacial layer in which macromolecules of different polymers are combined. Homopolymer PVAc has one structural glass transition at $T_{E''\max}$ = 34 °C. For PVAc/

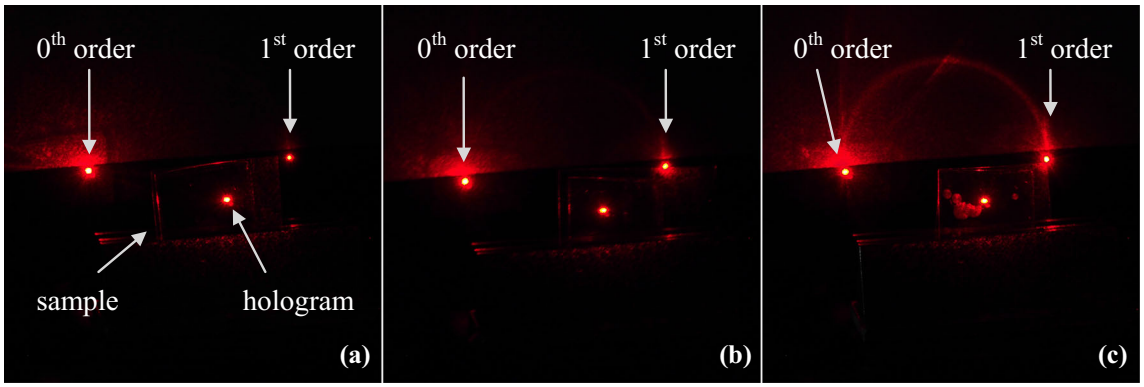

Figure 11 Photos of diffraction patterns of holograms recorded in photopolymers with DO monomer (**a**), OT monomer (**b**), and DT monomer (**c**). Zero and first diffraction orders, holograms, experimental samples are marked.

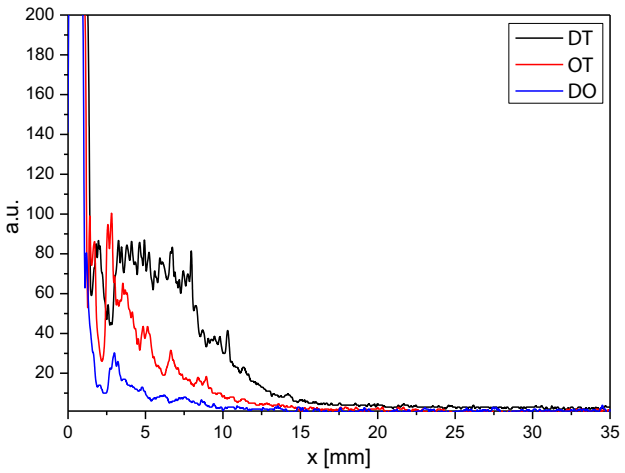

Figure 12 Relative scattered light intensity in the region of zero diffraction order for photopolymers with different monomers. (x = 0 is the center of zero-order beam).

OT and PVAc/DT films, two glass transitions are defined, for PVAc/DO films, three transitions are defined. The results obtained indicate phase separation in mixed films during UV polymerization of new monomers in a PVAc binder.

The data obtained for the DO polymer in the polyvinyl acetate binder showed the presence of three peaks on the graphs of the $E''(T)/tg\delta(T)$ (Fig. 13), which correspond to three glass transition temperatures: 46/50, 63/68, and 118/126 °C (Table 3). This suggests that three phases are formed. T_g = 46/50 °C corresponds to polyvinyl acetate (T_g = 34/52 °C, Table 3), T_g = 63/68 °C corresponds to a homogeneous structure consisting of polyvinyl acetate and DO polymer, and T_g = 118/126 °C corresponds to DO homopolymer in polyvinyl acetate (T = 139 °C, Table 3).

In the case of the OT polymer in the polyvinyl acetate binder, two peaks were observed on the E''(T)/tgδ(T) plot with temperatures of 16/44 and 76/89 °C. Temperature T_g = 16/44 °C corresponds to polyvinyl acetate. Temperature T_g = 76/89 °C corresponds to a homogeneous structure consisting of polyvinyl acetate and OT polymer.

Similarly, two peaks were observed for the $E''(T)/tg\delta(T)$ DT plot of the polymer in the polyvinyl acetate binder. At 53/62 °C, the peak corresponds to a homogeneous structure consisting of polyvinyl acetate and DT polymer, and at T_g = 138 °C, the peak corresponds to DT homopolymer in polyvinyl acetate (T = 155 °C, Table 3).

Films consisting of polyvinyl acetate and newly formed DO polymer showed three glass transition temperature transitions, including a transition associated with the formation of a significant fraction of the interphase layer in which macromolecules of different polymers are combined. This indicates good compatibility between the polyvinyl acetate and the DO polymer. At the same time, films consisting of polyvinyl acetate and newly formed OT and DT polymers show two glass transition temperatures corresponding to the T_g of polyvinyl acetate and the new polymer. This indicates the absence of a homogeneous single-phase morphology of these films. Such an inhomogeneous structure of photopolymer holograms allows us to assert that the scattering of linearly polarized light on them is Rayleigh Scattering Regime and is determined by the expression [36]:

$$I = I_0 \frac{1+\cos^2\theta}{2R^2}\left(\frac{2\pi}{\lambda}\right)^4\left(\frac{m^2-1}{m^2+2}\right)^2\left(\frac{d}{2}\right)^6 \quad (3)$$

where I_0 is the incident radiation intensity, R is the distance of the observation point from the scattering

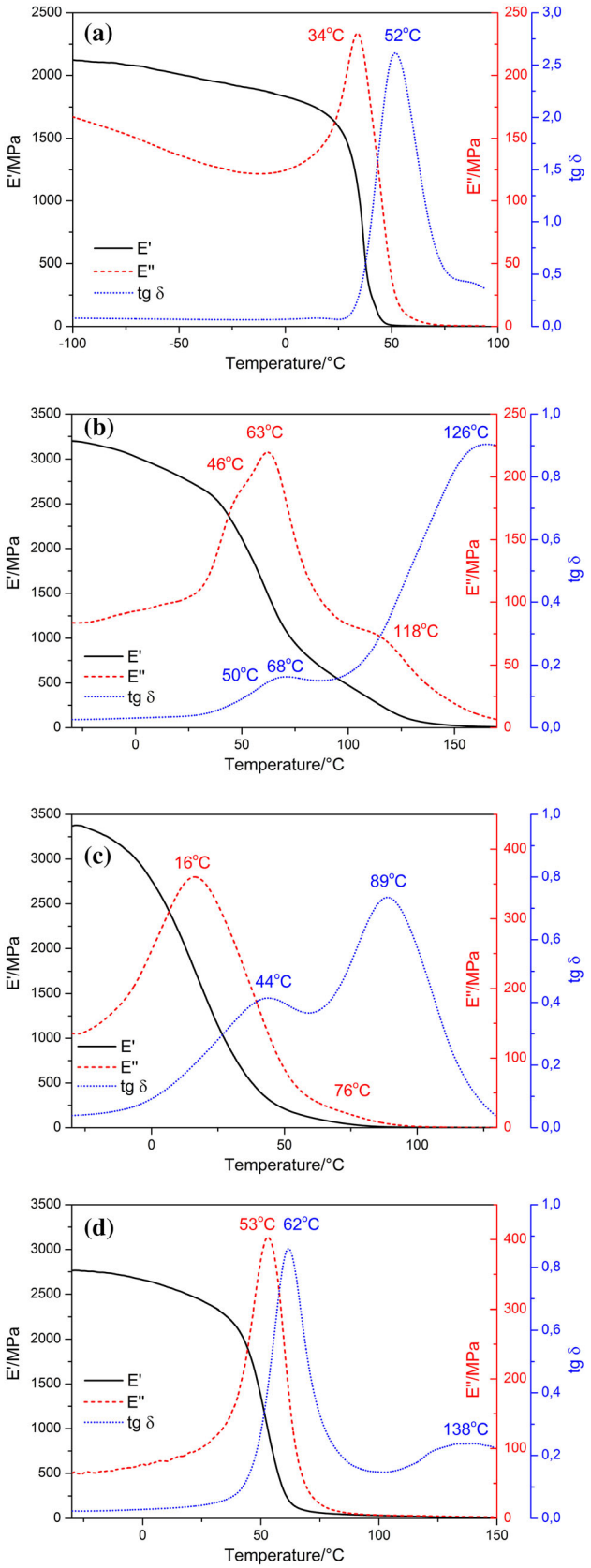

◀**Figure 13** Elastic modulus *E*', loss modulus *E*'', tangent of the angle of mechanical losses *tgδ* dependences on temperature for films **a** PVAc, **b** DO polymer—PVAc 50/50% wt., **c** OT polymer—PVAc 50/50% wt., **d** DT polymer—PVAc 50/50% wt.

volume, θ is the scattering angle, λ is the wavelength of linearly polarized light in the medium, d is the diameter of small spheres (in our case it is polymer scatter centers), $m = n_p/n_s$, where n_p and n_s are the refractive indices of the polymer and of the surrounding medium.

According to expression (3), the scattered light intensity is affected by the parameter m—the ratio between the RI of the newly formed polymer scatter centers and the polymer binder.

The parameter m (the ratio between the RI of the formed polymer scatter centers and the polymer binder) affects the scattered light intensity according to expression (3). The ratio of RIs of the DO polymer and polyvinyl acetate is $m = 1.05$, OT polymer and polyvinyl acetate: $m = 1.08$, and DT polymer and polyvinyl acetate: $m = 1.11$. This leads to an increase in light scattering for the OT polymer by a factor of 2.6, and for the DT polymer by a factor of 4.7 in comparison with the DO polymer. This dependence corresponds to the data shown in Fig. 12. The integral area under the curves of the relative scattered light intensity (Fig. 12) is approximately 100, 300, and 500 units·mm. Thus, the approach to the development of HPM, which uses a polymer binder with a low RI and a monomer with a high RI, may have a natural limitation associated with an increase in light scattering when using incompatible polymer structures.

Another factor that can affect the increase in light scattering is an increase in the average scatter center diameter of the polymer formed in the binder during photopolymerization. The van der Waals radius of the sulfur atom is about 1.2 times larger than the oxygen radius, as well as the carbon–sulfur bond ~ 1.2 times the length of the carbon–oxygen bond, which leads to the formation of larger polymer scatter centers and, as a result, to an increase in light scattering.

In addition, the formation of crosslinks due to the formation of disulfide bridges is possible for sulfur-

Table 3 Glass transition temperatures of the studied polymer films measured by DMA

Film	The glass transition #1		The glass transition #2		The glass transition #3	
	$T_{E''max}$, °C	$T_{tg\delta}$, °C	$T_{E''max}$, °C	$T_{tg\delta}$, °C	$T_{E''max}$, °C	$T_{tg\delta}$, °C
DO	139*	–	–	–	–	–
OT	130*	–	–	–	–	–
DT	155*	–	–	–	–	–
PVA	34	52	–	–	–	–
PVA/DO	46	50	63	68	118	126
PVA/OT	16	44	76	89	–	–
PVA/DT	53	62	–	–	n/a	138

*The glass transition temperatures measured by DSC

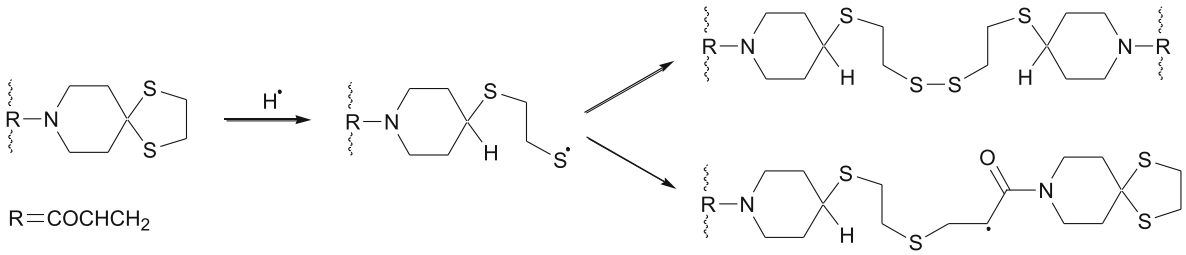

Scheme 1 –S–S– and –S–C– crosslink formation.

containing compounds. The reaction is typical for thiols and organic cyclic disulfides [37]. Sulfur crosslinks can occur in the case of photopolymerization of OT and DT monomers. However, the formation of the crosslinked polymer will proceed most efficiently for the DT monomer with two sulfide groups. During photopolymerization, both –S–S– and –S–C– crosslinks can form, as shown in Scheme 1.

In a crosslinked polymer, firstly, the diffusion of monomer molecules to radical centers on polymer chains is significantly reduced and the growth of an acrylamide-type polymer is inhibited. In the literature, the importance of free diffusion of monomer molecules for the effective growth of polymer structures during holographic gratings recording has been shown [38]. A decrease of the monomer molecules diffusion substantially limited of polymerization reaction and leads to decrease of DE of holograms. This negative effect, combined with increased light scattering, reduces the positive effect of increasing the difference between the RIs of the binder and the polymer. Crosslinks also lead to an increase of the diffusion limitations and scatter center diameter of the polymer and as result to an increase in light scattering.

Conclusions

The replacement of two oxygen atoms by sulfur atoms allows to increase RI of the polymer from 1.5433 (DO) to 1.630 (DT). Taking into account $n_{poly(vinyl\ acetate)}$ = 1.467, the difference in RI between the formed polymer and the binder increased 2.1 times from 0.076 to 0.163. Doubling the difference in RI allowed expecting a doubling of n_1 too, but real increase of n_1 was 1.25 times during holographic recording. The estimates made showed that the main reasons for this discrepancy may be a decrease in the macrodiffusion of the monomer in the binder and an increase in light scattering by the formed diffraction gratings. Studies of polymers based on spirocyclic acryloyl derivatives of 4-piperidone with oxygen and sulfur atoms in the spirocycles have been carried out to study this phenomenon. The type of spirocycle affects the size of scatter centers and their efficiency, as well as the features of the formation of interpenetrating polymer networks in HPM. The thermomechanical, refractive, optical, and holographic properties depend on the type of the spirocyclic (–O–CH_2–CH_2–O–, –O–CH_2–CH_2–S–, –S–CH_2–CH_2–S–) too. Particular attention should be paid to the compatibility of the new polymer and binder. This is most

clearly manifested for the studied HPM: DT polymer in a polyvinyl acetate matrix. Apparently, polyvinyl acetate does not have sufficient free volume for the introduction of the polymer network of the DT polymer. Decrease in the compatibility of the polyvinyl acetate binder with sulfur-containing photopolymers confirmed by the DMA method. This in turn leads to an increase in light scattering.

This observation suggests that the approach aimed at increasing the efficiency of the HPM by using sulfur-containing high RI polymers requires taking into account their phase morphological compatibility with the polymer binder.

Acknowledgements

Authors would like to acknowledge the Multi-Access Chemical Research Center SB RAS for spectral and analytical measurements. This research conducted under a scientific theme FWUE-2022-0016 and 122040400028-5 and did not receive any specific grant from funding agencies in the public, commercial, or not-for-profit sectors.

Data availability

The raw/processed data required to reproduce these findings cannot be shared at this time as the data also forms part of an ongoing study.

Declaration

Conflict of interest All authors certify that they have no affiliations with or involvement in any organization or entity with any financial interest or non-financial interest in the subject matter or materials discussed in this manuscript.

References

[1] Blanche PA, Bablumian A, Voorakaranam R, Christenson C, Lin W, Gu T, Flores D, Wang P, Hsieh W-Y, Kathaperumal M, Rachwal B, Siddiqui O, Thomas J (2010) Holographic three-dimensional telepresence using large-area photorefractive polymer. Nature 468:80–83

[2] Sheeja MK, Ajith Kumar PT, Nair Achuthsankar S (2006) Photopolymer based holographic variable data storage system for security applications.In: Proceedings of SPIE 6352, 635224

[3] Hesselink L, Orlov S, Bashaw MC (2004) Holographic data storage systems. Proc IEEE 92(8):1231–1280

[4] Zanutta A, Orselli E, Fäcke T, Bianco A (2016) Photopolymer based VPHGs: from materials to sky results. Proc SPIE 9912:99123B-B99131

[5] Pen EF (2019) Energy efficiency of photovoltaic panels when using holographic gratings as passive solar trackers. Optoelectron Instrum Data Process 55(3):271–279

[6] Blanche P-A (2020) Optical holography-materials, theory and applications. Holographic Recording Media Devices, pp 41–60.https://doi.org/10.1016/B978-0-12-815467-0.00002-5.

[7] Malallah R, Li H, Kelly DP, Healy JJ, Sheridan JT (2017) A review of hologram storage and self-written waveguides formation in photopolymer media. Polymers 9:337–371. https://doi.org/10.3390/polym9080337

[8] Vasilyev EV, Shelkovnikov VV, Orlova NA, Steinberg ISh, Loskutov VA (2020) Single- and two-photon recording of holograms at combined catio2012 nic and free-radical polymerization photoinitiated by thioxanthenone derivatives. Polym J 52(11):1279–1287

[9] Crivello JV, Lam JHW (1996) Photoinitiated cationic polymerization with triarylsulfonium salts. J Pol Sci Part A Pol Chem 34:3231–3253.

[10] J.V. Crivello, The Discovery and Development of Onium SaltCationic Photoinitiators, J. Pol. Sci.: Part A: Pol. Chem. 37 (1999) 4241–4254.

[11] Gomez ML, Previtali CM, Montejano HA (2012) Two- and three-component visible light photoinitiating systems for radical polymerization based on onium salts: an overview of mechanistic and laser flash photolysis studies. Int J Photoenergy Article ID 260728:1–9

[12] Kitano H, Ramachandran K, Scranton AB (2012) Free radical shadow cure initiated using two-component and three-component initiator systems. Int J Photoenergy Article ID 213846:1–8

[13] Gomez ML, Montejano HA, Bohorquez MV, Previtali CM (2004) Photopolymerization of acrylamide initiated by the three-component system safranine/triethanolamine/diphenyliodonium chloride: the effect of the aggregation of the salt. J Polymer Sci A Polym Chem 42:4916–4920

[14] Hassoon S, Neckers DC (1995) Electron transfer photoreduction of 5,7-Diiodo-3-butoxy-6-fluorone with tetrabutylammonium triphenylborate and N, N-dimethyl-2,6-diisogropylaniline. J Phys Chem 99:9416–9424

[15] Gomez ML, Previtali CM, Montejano HA (2007) Phenylonium salts as third component of the photoinitiator system Safranine O/triethanolamine: a comparative study in aqueous media. Polymer 48:2355–2361

[16] Kogelnik H (1969) Coupled wave theory for thick hologram gratings. Bell Syst Tech J 48(9):2909–2947. https://doi.org/10.1002/j.1538-7305.1969.tb01198.x

[17] Alim MD, Glugla DJ, Mavila S, Wang C, Nystrom PD, Sullivan AC, McLeod RR, Bowman CN (2018) High dynamic range (Δn) two-stage photopolymers via enhanced solubility of a high refractive index acrylate writing monomer. ACS Appl Mater Interfaces 10:1217–1224. https://doi.org/10.1021/acsami.7b15063

[18] Hu Y, Kowalski BA, Mavila S, Podgórski M, Sinha J, Sullivan AC, McLeod RR, Bowman CN (2020) Holographic photopolymer material with high dynamic range (Δn) via Thiol-Ene click chemistry. ACS Appl Mater Interfaces 12:44103–44109

[19] Higashihara T, Ueda M (2015) Recent progress in high refractive index polymers. Macromolecules 48:1915–1929

[20] Dèsilles N, Gautrelet C, Lecamp L, Lebaudy P, Bunel C (2005) Effect of UV light scattering during photopolymerization on UV spectroscopy measurements. Euro Polymer J 41:1296–1303.

[21] Basistyi VS, Bukhtoyarova AD, Vasil'ev EV, Shelkovnikov VV (2018) Monomers with a High Refraction Index Based on Acryloyl derivatives of spirocyclic piperidin-4-one thioacetals. Opt Spectrosc 125:82–87. https://doi.org/10.1134/S0030400X18070044.

[22] Sola R, Brugidou J, Taillades J, Commeyras A, Previero A (1983) Composes cetoniques supportes catalyseurs d'hydratation des α-aminonitriles. Tetrahedron Lett 24(14):1501

[23] Loskutov VA, Shelkovnikov VV (2006) Synthesis of hexafluorophosphates of 9-oxo-10-(4-heptoxyphenyl)thioxanthenium. Russ J Org Chem 42:298

[24] Ioffe BV (1960) Refractometry as a method for the physicochemical analysis of organic systems. Russ Chem Rev 29:53

[25] Lawrence JR, O'Neill FT, Sheridan JT (2001) Photopolymer holographic recording material. Optik 112(10):449–463

[26] Xueping G, Qiang Y, Song L, Misra A, Spencer P (2015) Visible-light initiated free-radical/cationic ring-opening hybrid photopolymerization of methacrylate/epoxy: polymerization kinetics, crosslinking structure, and dynamic mechanical properties. Macromol Chem Phys 216:856

[27] Song L, Ye Q, Ge X, Misra A, Tamerlerac C, Spencer P (2016) Self-strengthening hybrid dental adhesive via visible-light irradiation triple polymerization. RSC Adv 6:52434

[28] Murugan R, Mohan S, Bigotto A (1998) FTIR and polarised Raman spectra of acrylamide and polyacrylamide. J Korean Phys Soc 32(4):505512

[29] Dreiera TA, Ringstranda BS, Seifertb S, Firestone MA (2018) Synthesis and application of a metal ion coordinating ionic liquid monomer: towards size and dispersity control of nanoparticles formed within a structured polyelectrolyte. Eur Polymer J 107:275–286

[30] Feng L, Yang H, Dong X, Lei H, Chen D (2018) pH-sensitive polymeric particles as smart carriers for rebar inhibitors delivery in alkaline condition. J Appl Polym Sci 135(8):45886. https://doi.org/10.1002/APP.45886

[31] Vasilyev EV, Shelkovnikov VV, Orlova NA, Steinberg ISh, Loskutov VA (2020) Single- and two-photon recording of holograms at combined cationic and free-radical polymerization photoinitiated by thioxanthenone derivatives. Polymer J 52:1279–1287. https://doi.org/10.1038/s41428-020-0381-2

[32] Shelkovnikov VV, Loskutov VA, Vasil´ev EV, Shekleina NV, Ryabinin VA, Sinyakov AN (2011) New acid photogenerators based on thioxanthen-9-one sulfonium derivatives for detritylation in the oligonucleotide synthesis. Russ Chem Bull Int Ed. 60: 561. https://doi.org/10.1007/s11172-011-0087-x

[33] Shim H, Monticone F, Miller OD (2021) Fundamental limits to the refractive index of transparent optical materials. Adv Mater 33:2103946

[34] Utsugi T (2018) Holographic scattering in an angular-multiplexed hologram on a photopolymer. Appl Opt 57(3):527–537

[35] McLeod RR (2020) Numerical technique for study of noise grating dynamics in holographic photopolymers. Polymers 12:2744. https://doi.org/10.3390/polym12112744

[36] Piazza R, Degiorgio V (2005) Scattering, Rayleigh. Encyclopedia Condens Matter Phys, pp 234–242. https://doi.org/10.1016/b0-12-369401-9/00648-3

[37] Beaupre DM, Weiss RG (2021) Thiol- and disulfide-based stimulus-responsive soft materials and self-assembling systems. Molecules 26:3332. https://doi.org/10.3390/molecules26113332

[38] Piazzolla S, Jenkins BK (2000) First-harmonic diffusion model for holographic grating formation in photopolymers. J Opt Soc Am 17(7):1147–1157